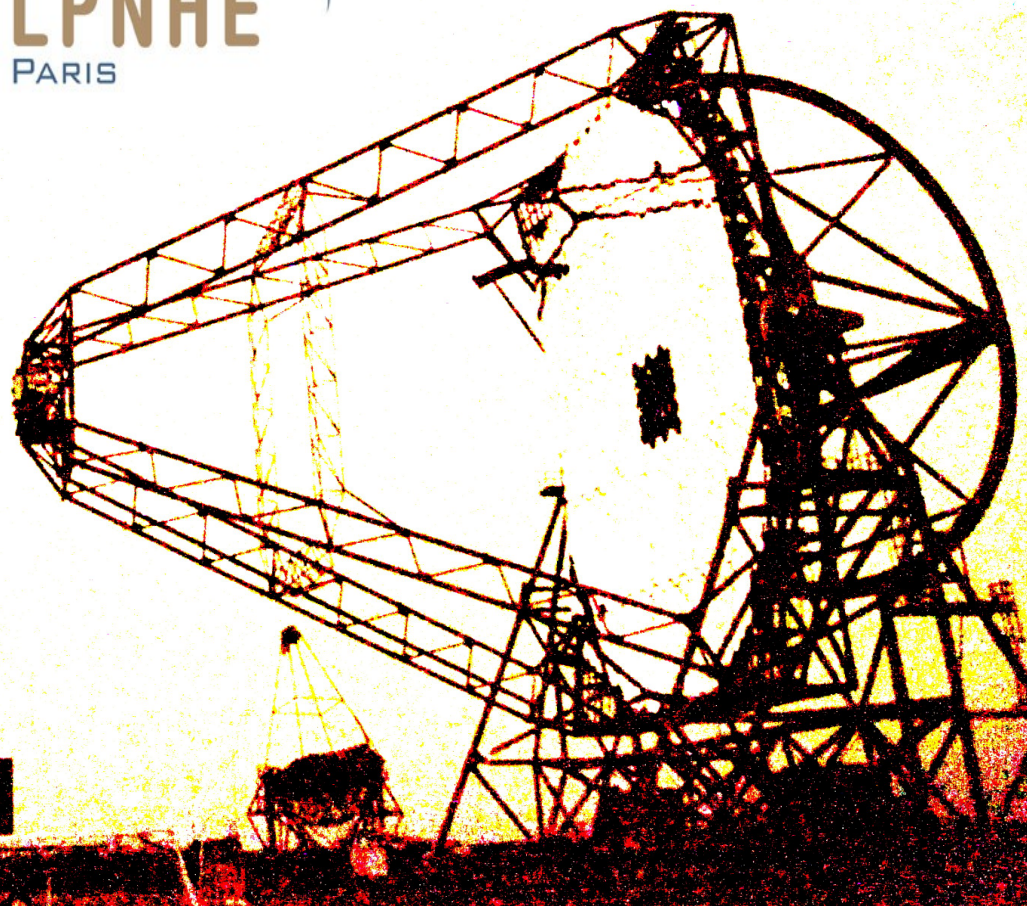


# LIV studies with HESS II



**M. Chrétien  
J. Bolmont  
A. Jacholkowska  
C. Couturier**



**2<sup>nd</sup> OKC DIAS Workshop, Stockholm, 23-25 October 2013**

# Outline

**LIV in Fundamental Theories**

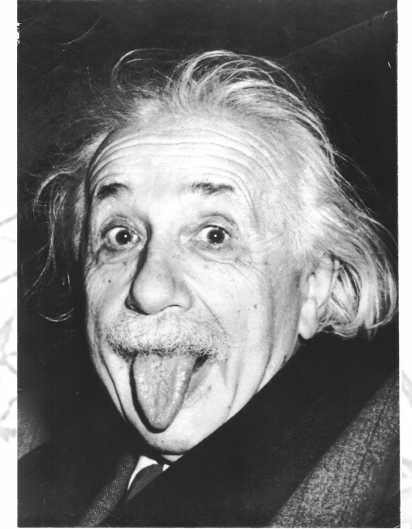
**LIV tests with Cherenkov Telescopes**

**HESS II performance: Monte Carlo Studies**

**Summary and Conclusions**

# LIV in Fundamental Theories

- **Lorentz Invariance/Symmetry:** Einstein's Relativity & Standard Model
- At Planck scale  $\sim 10^{-35}$  m ( $10^{19}$  GeV), nature of space-time needs to account for microscopic effects
  - **Quantum Gravity (QG)**
- Some models of QG lead to **Lorentz Invariance Violation**
  - D branes String model (foamy structure of space-time)
  - Non-commutative geometry
  - Spontaneous symmetry breaking (SME)
  - LQG
  - ...
- LIV can be tested in different ways:
  - Photon decay, Vacuum Cherenkov Radiation
  - Modified GZK cutoff, and TeV  $\gamma$ -ray spectra of extra-galactic sources.
  - Vacuum birefringence
  - **Dispersion of light in vacuum**



# Modification of dispersion relations in vacuum

- LIV modifies dispersion relation for the photon:

$$c^2 p^2 = E^2 \left( 1 + \xi \left( \frac{E}{E_{\text{planck}}} \right) + \zeta \left( \frac{E}{E_{\text{planck}}} \right)^2 + \dots \right)$$

- Leading order corrections to the speed of light ( $c$ ) in vacuum:

$$v = \delta E / \delta p = c \left( 1 - \xi \left( \frac{E}{E_{\text{planck}}} \right) - \zeta \left( \frac{E}{E_{\text{planck}}} \right)^2 \right)$$

$$\xi = \frac{E_{\text{planck}}}{E_{\text{QG}}} \quad \text{and} \quad \zeta = \left( \frac{E_{\text{planck}}}{E_{\text{QG}}} \right)^2 \quad \text{are LIV parameters } (<0 \text{ or } >0)$$

- Figure of merit of LIV:

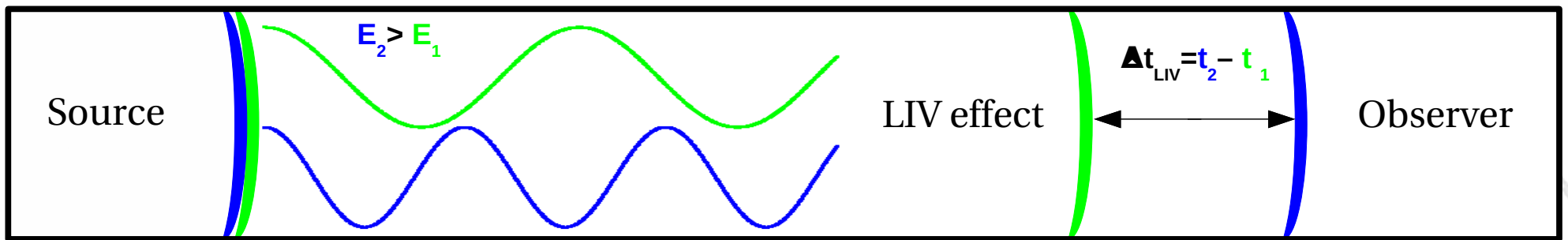
$$\xi \approx \frac{c E_p \Delta t}{d \Delta E}$$

**Best sensitivity for :**  
Fast variability sources  
Distant sources  
Energetic sources

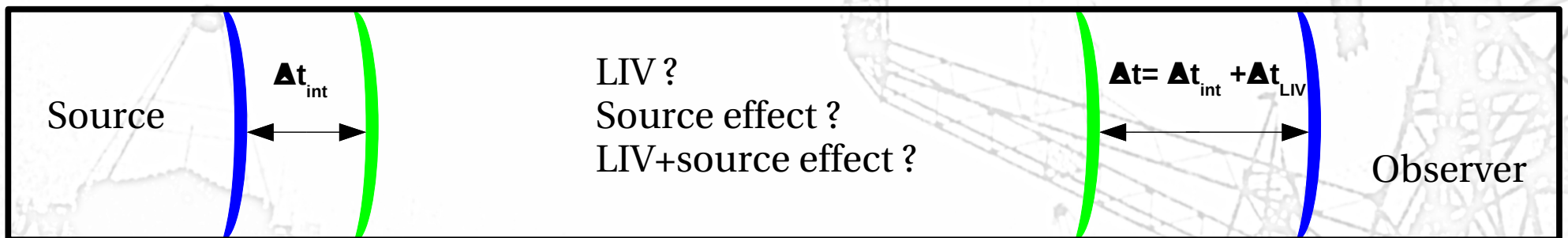
superluminal      subluminal

# Vacuum dispersion

- 2 photons of energies  $E_1$  and  $E_2 (>E_1)$  emitted at time  $t$
- observed with a relative  $\Delta t_{LIV} = t_2 - t_1$  ( $>0$  for subluminal,  $<0$  for superluminal)



- Possible source intrinsic delays

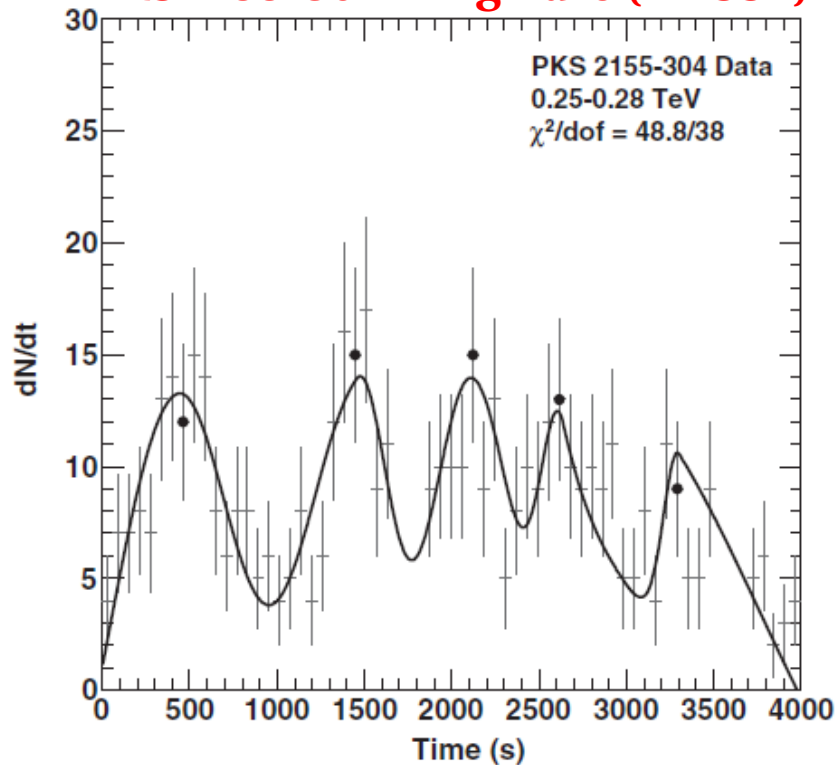


- Source effect is major caveat : only redshift dependence study can distinguish

# LIV tests with Cherenkov Telescopes

- Energy dispersion of time of arrivals in observed gamma rays.

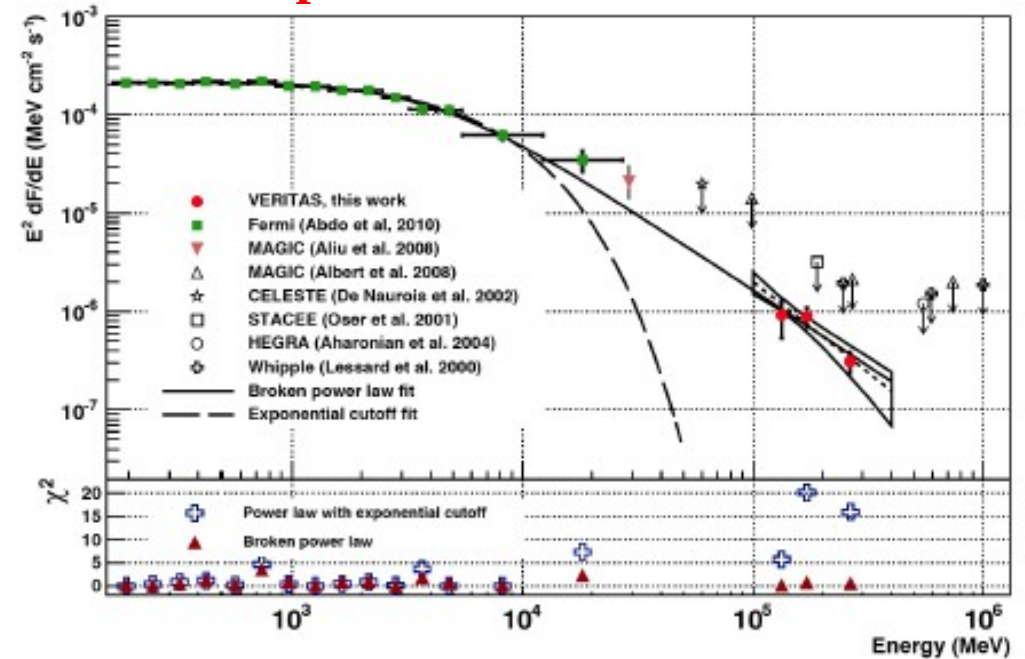
## PKS2155-304 – Big flare (HESS I)



$$E_{QG,l} > 2.1 \times 10^{18} \text{ GeV}$$

Maximum Likelihood method  
Astroparticle Physics 34 (2011) 738–747

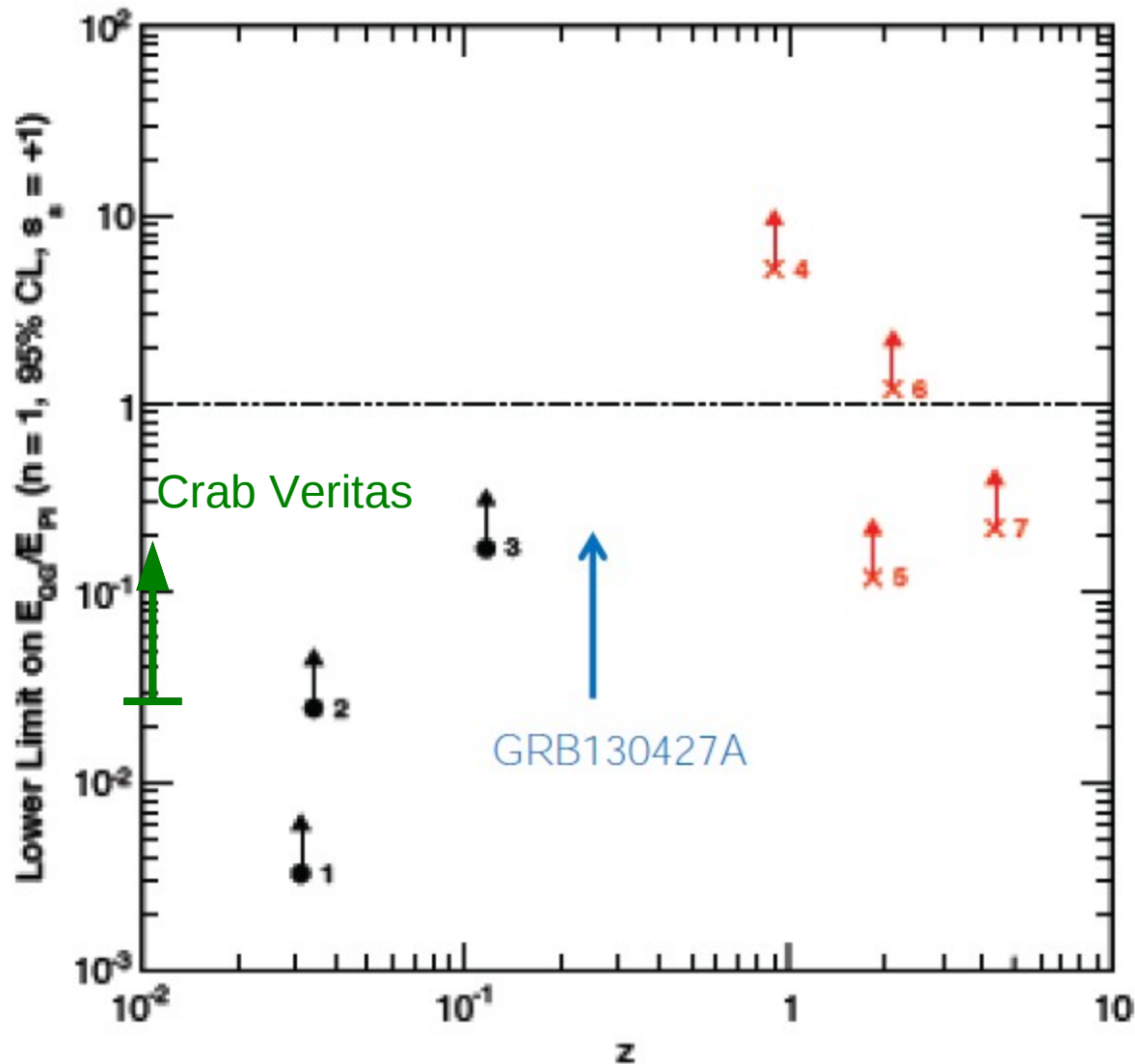
## Crab-pulsed emission (VERITAS)



$$E_{QG,l} > 1.9 \times 10^{17} \text{ GeV}$$

DisCan method  
arXiv:1307.8382v1 [astro-ph.HE] 31 Jul 2013

# Present QG limits on linear term



- Apart from large redshift GRBs & PKS 2155-304 , Crab pulsar good competitor.

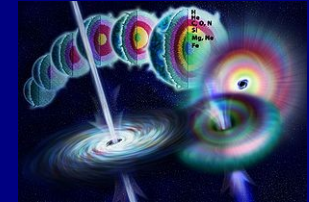
# Astrophysical probes of LIV with HESS II



**Pulsar**



**Active Galactic Nuclei**



**Gamma Ray Burst**

	<b>Pulsar</b>	<b>Active Galactic Nuclei</b>	<b>Gamma Ray Burst</b>
<b>Ad.</b>	<ul style="list-style-type: none"> <li>• Permanent pulsations</li> <li>• Distinguish between LIV/source effects</li> </ul>	<ul style="list-style-type: none"> <li>• Extragalactic</li> <li>• Up to TeV</li> </ul>	<ul style="list-style-type: none"> <li>• Extragalactic</li> <li>• Up to TeV?</li> </ul>
<b>Disad.</b>	<ul style="list-style-type: none"> <li>• Galactic</li> <li>• Up to 400 GeV(Crab) to be confirmed with H.E.S.S.2</li> </ul>	<ul style="list-style-type: none"> <li>• Source effects</li> <li>• Random transient evts</li> </ul>	<ul style="list-style-type: none"> <li>• Source effects</li> <li>• Obs. based on luck</li> </ul>
<b>HESS II running mode</b>	<ul style="list-style-type: none"> <li>• Mono</li> <li>→ Access lower energies (crucial with pulsars)</li> </ul>	<ul style="list-style-type: none"> <li>• Hybrid</li> <li>→ Access higher energies (crucial with AGNs)</li> </ul>	<ul style="list-style-type: none"> <li>• Hybrid</li> </ul>

# The method of time-lag measurement

- Strategy adapted from *Martinez & Errando (Astropart.Phys. 31 (2009) 226)*

$$P(E, t) = N \int_0^\infty A(E_s) \Gamma(E_s) G(E - E_s, \sigma(E_s)) F_s(t_s - \tau_n E_s^n) dE_s$$

$A(E_s)$ : Acceptance of telescope

$\Gamma(E_s)$ : Spectrum at source

$G(E - E_s)$ : Energy smearing function

$F_s(t_s)$ : Light curve at source

- The **time-lag parameter** :  
(s/TeV for n=1)  
(s/TeV<sup>2</sup> for n=2)

$$\tau_n = \frac{\Delta t}{\Delta E} \approx \frac{(n+1)\xi}{2E_p^n H_o} \int_0^z \frac{(1+z)}{\sqrt{\Omega_m (1+z)^3 + \Omega_\Lambda}} dz$$

- 1) Parametrize Template Light curve  $F_s(t_s)$  at **low energy** and spectrum  $A(E_s)$
- 2) Use **Maximum Likelihood** at **high energy** to estimate the **time lag parameter**.

- The likelihood is the product of the p.d.f's over all the photons in the fit:

$$L = \prod_i P(E, t)$$

# HESS II performances with pulsars

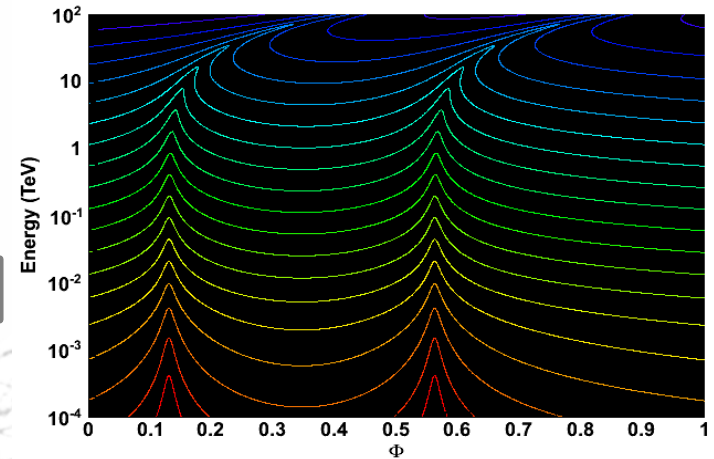
## The method

- Time delay due to LIV:  
→ **phase delay** between photons of  $\neq$  energies in the reconstructed phasogram.

- Define a **phase-lag parameter** :  
(TeV<sup>-1</sup> for n=1)  
(TeV<sup>-2</sup> for n=2)

$$\varphi_n = \frac{\tau_n}{P(t)}$$

$$P(t) \approx P + \dot{P}t \quad \text{For short time scale: } P(t) \approx P$$



- Parametrize Template Phasogram  $F_s$  at **low energy** and spectrum  $A(E_s)$

$$F_s(t_s - \tau_n E_s^n) \rightarrow F_s(\Phi_s - \varphi_n E_s^n)$$

$$P(E, t) \rightarrow P(E, \Phi)$$

- **Maximum Likelihood** at **high energy** gives estimate on the **phase-lag parameter**.

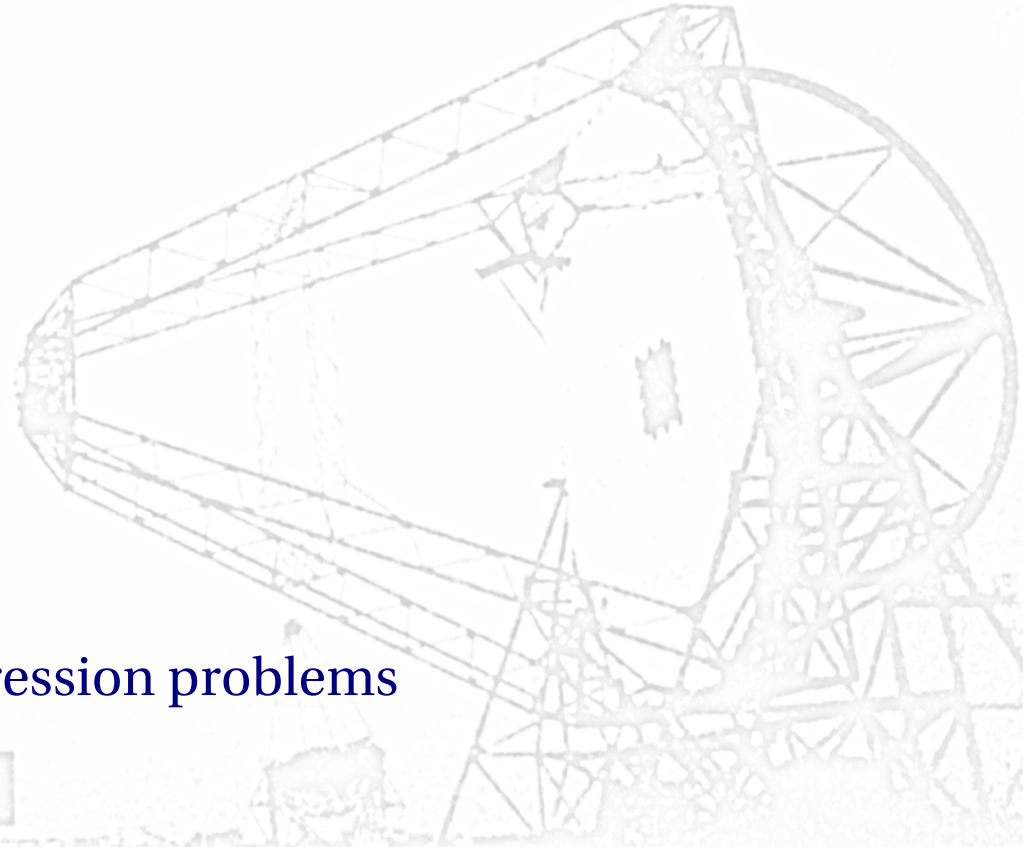
$$L = \prod_i P(E, \Phi)$$

# HESS II performances with pulsars

- 1 single pulse in phasogram
  - $\sigma_{\text{pulse}} = 2 \times 10^{-2}$  (rotational phases)
  - Power law spectrum  $E^{-\Gamma}$   $\Gamma=3.3$
- Acceptance & energy resolution
  - **H.E.S.S.2 mono**
  - $\Delta E/E \sim 35\%$
- 2 studies:
  - **B1 model:**  $S/B = \infty$  ( $>30$  GeV)
  - **B2 model:**  $S/B = 1$  ( $>30$  GeV)

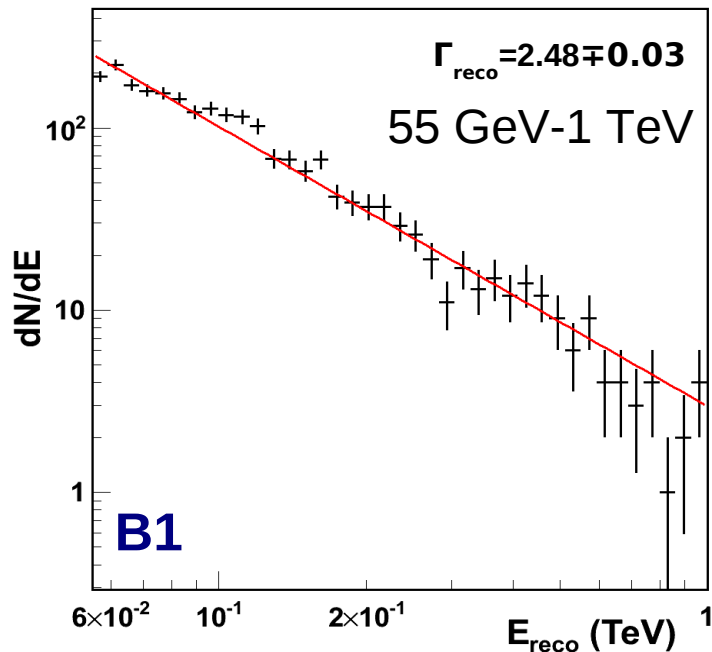
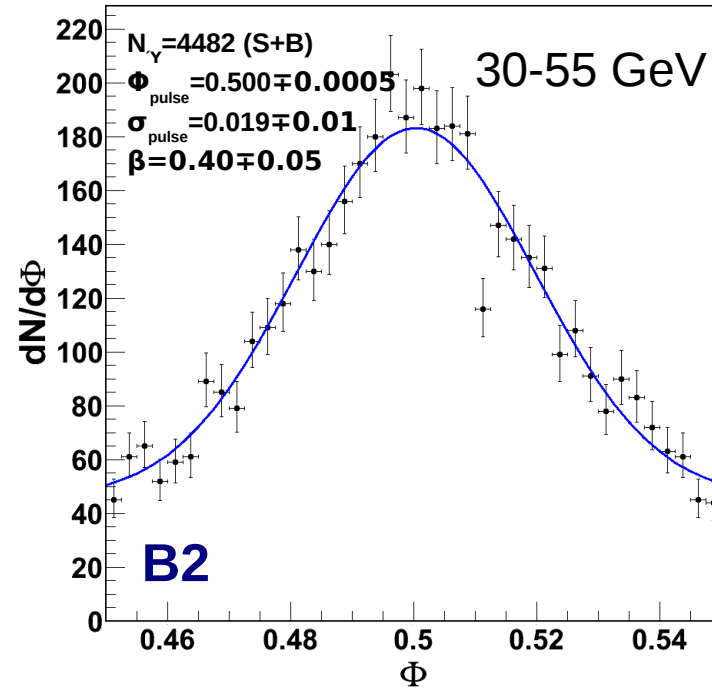
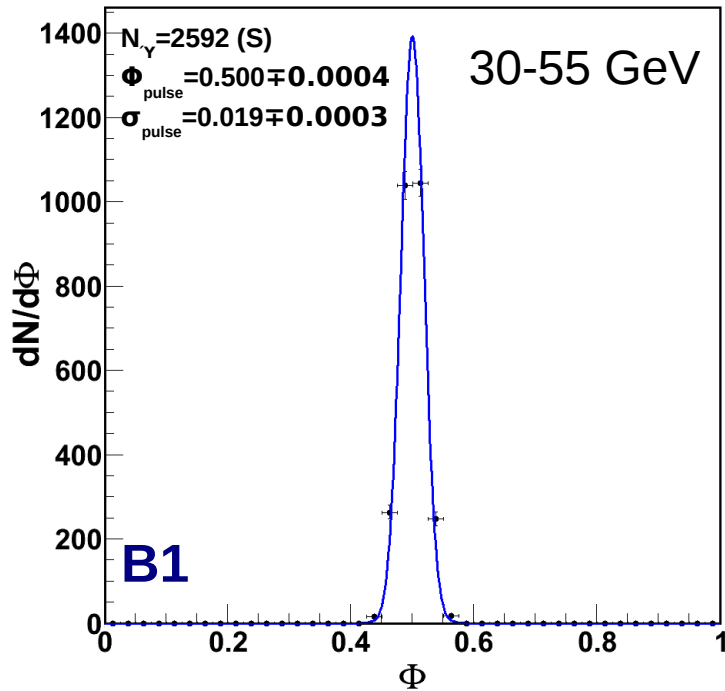
## Model is optimistic:

- Pulse shape not Gaussian
- $S/B$  could be  $>1$  due to hadron bckg suppression problems



# HESS II performances with pulsars

## Template phasogram and spectrum

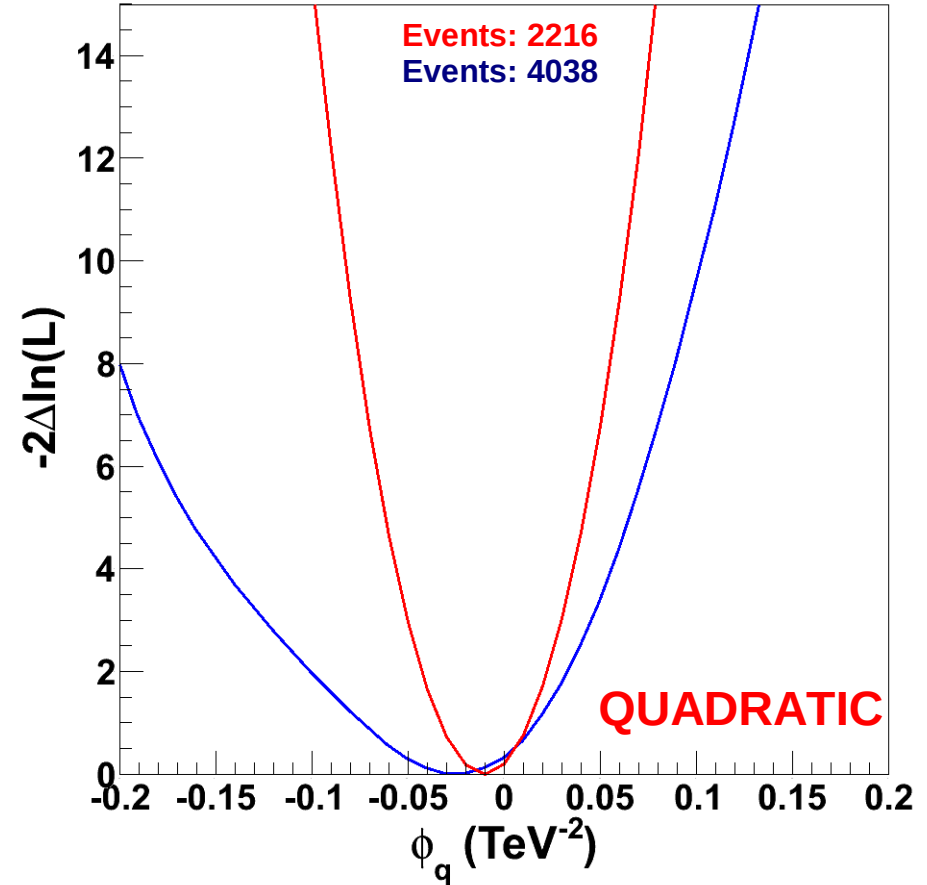
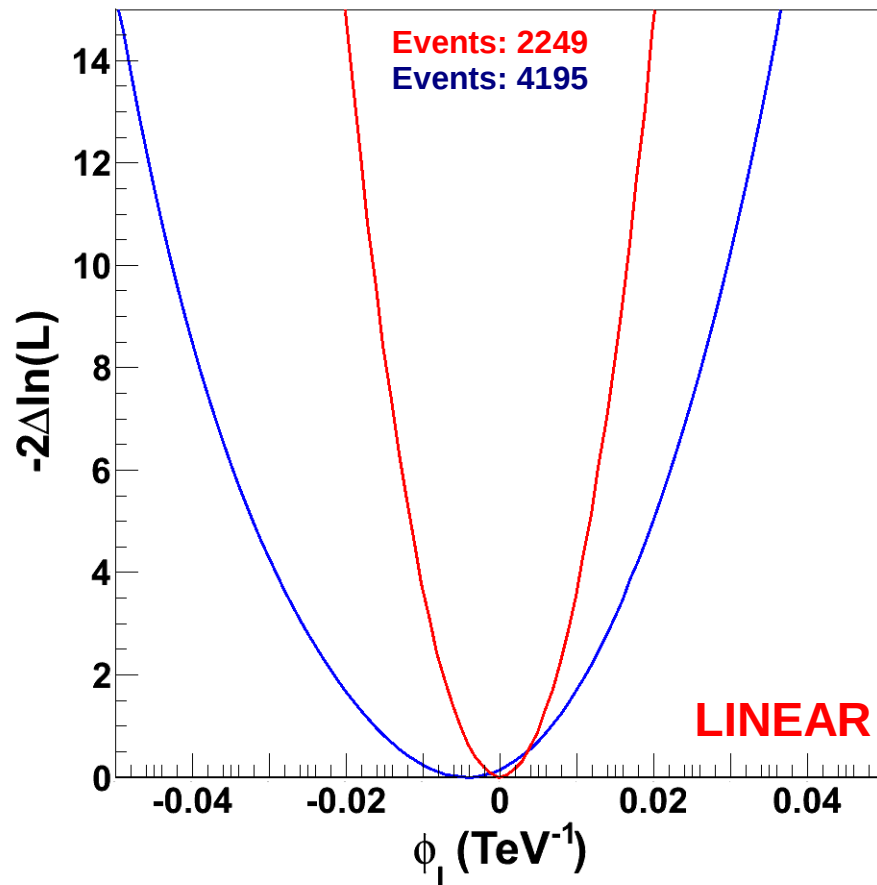


- **B1:  $S/B = \infty$ :**
  - Fit phasogram using Gaussian pulse.
  - Fit spectrum with power law (>55GeV)
- **B2:  $S/B = 1$ :**
  - Fit phasogram using  $(1-\beta) \times \text{Gaussian}(\Phi) + \beta \times \text{Uniform}(\Phi)$

# HESS II performances with pulsars

## Results

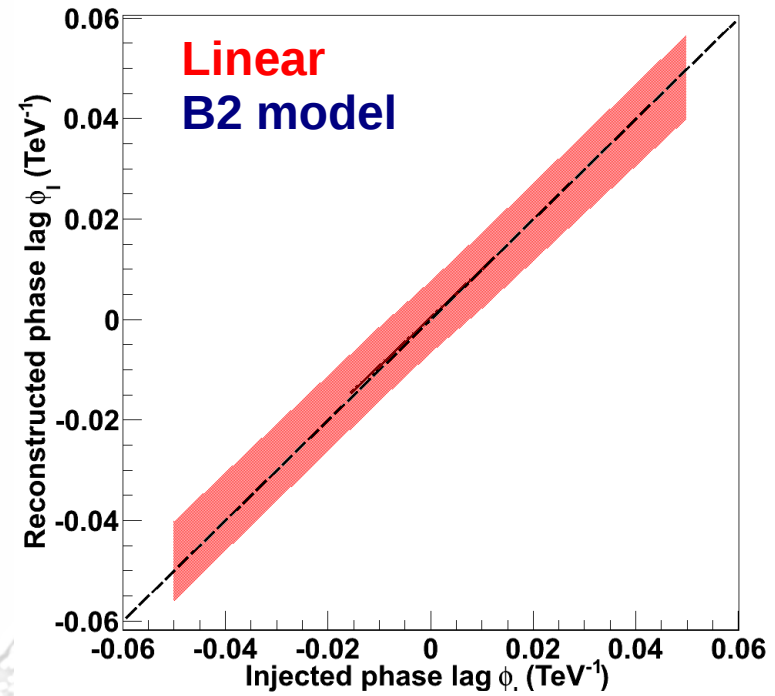
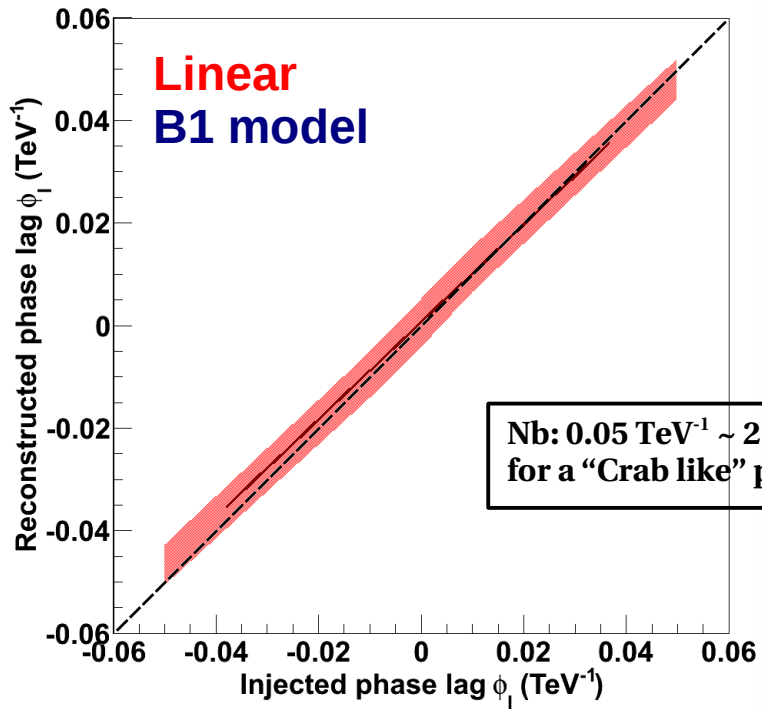
- Estimate on phase-lag parameter given by minimum of  $-2\Delta\ln(L)$ .



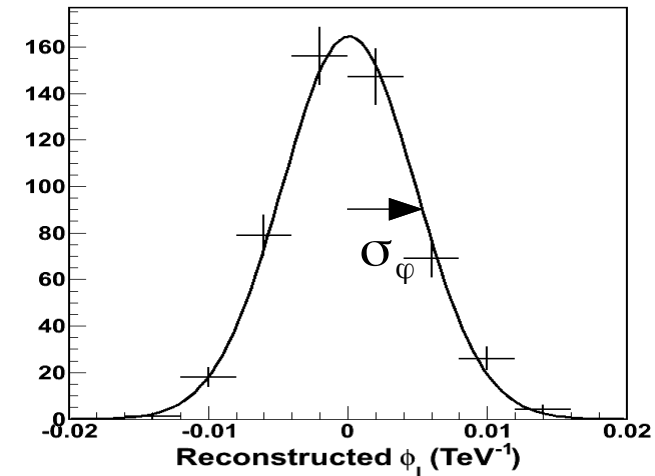
- **Red** : B1 model (no background)
- **Blue**: B2 model (S/B=1)
- Wider “parabola” due to background contamination.

# HESS II performances with pulsars

## Calibration of the method



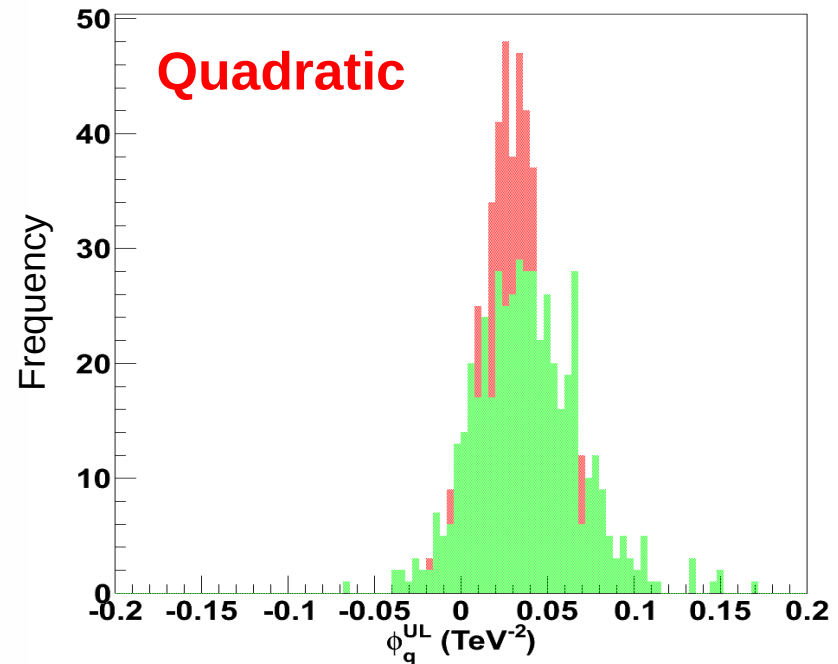
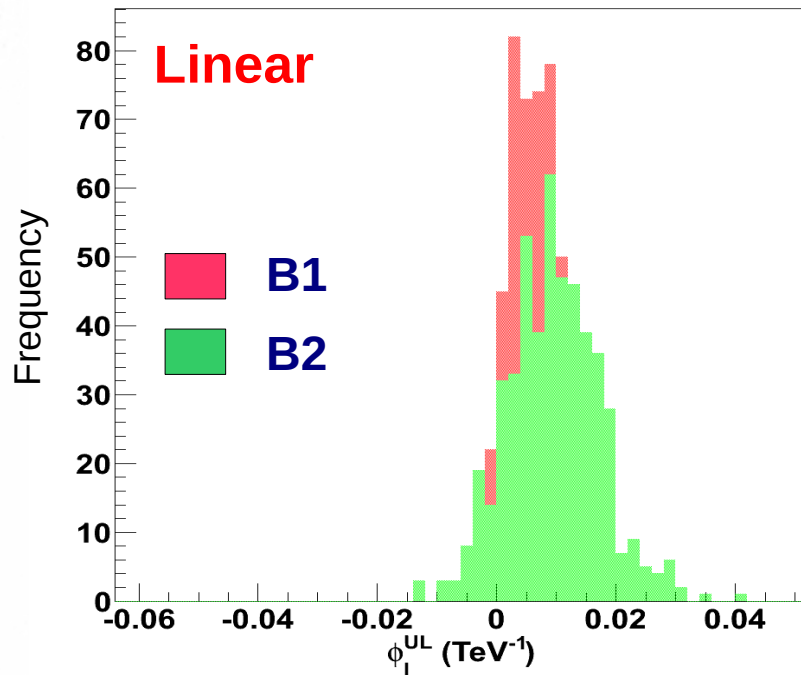
	$N_{\text{evt}}$	Calibrated error $\sigma_{\phi} (\varphi_{\text{inject}}=0)$	Remarks
Linear $S/B=\infty$	2449	$0.0047 \pm 0.0001$ $\text{TeV}^{-1}$	-
Linear $S/B=1$	4195	$0.0072 \pm 0.0002$ $\text{TeV}^{-1}$	~35% deterioration
Quadratic $S/B=\infty$	2216	$0.0193 \pm 0.0006$ $\text{TeV}^{-2}$	-
Quadratic $S/B=1$	4038	$0.0285 \pm 0.0006$ $\text{TeV}^{-2}$	~32% deterioration



# HESS II performances with pulsars

## Calibration of confidence intervals

- 95% CL upper/lower limits on phase lag parameter are derived from  $-2\Delta\ln(L)$ .



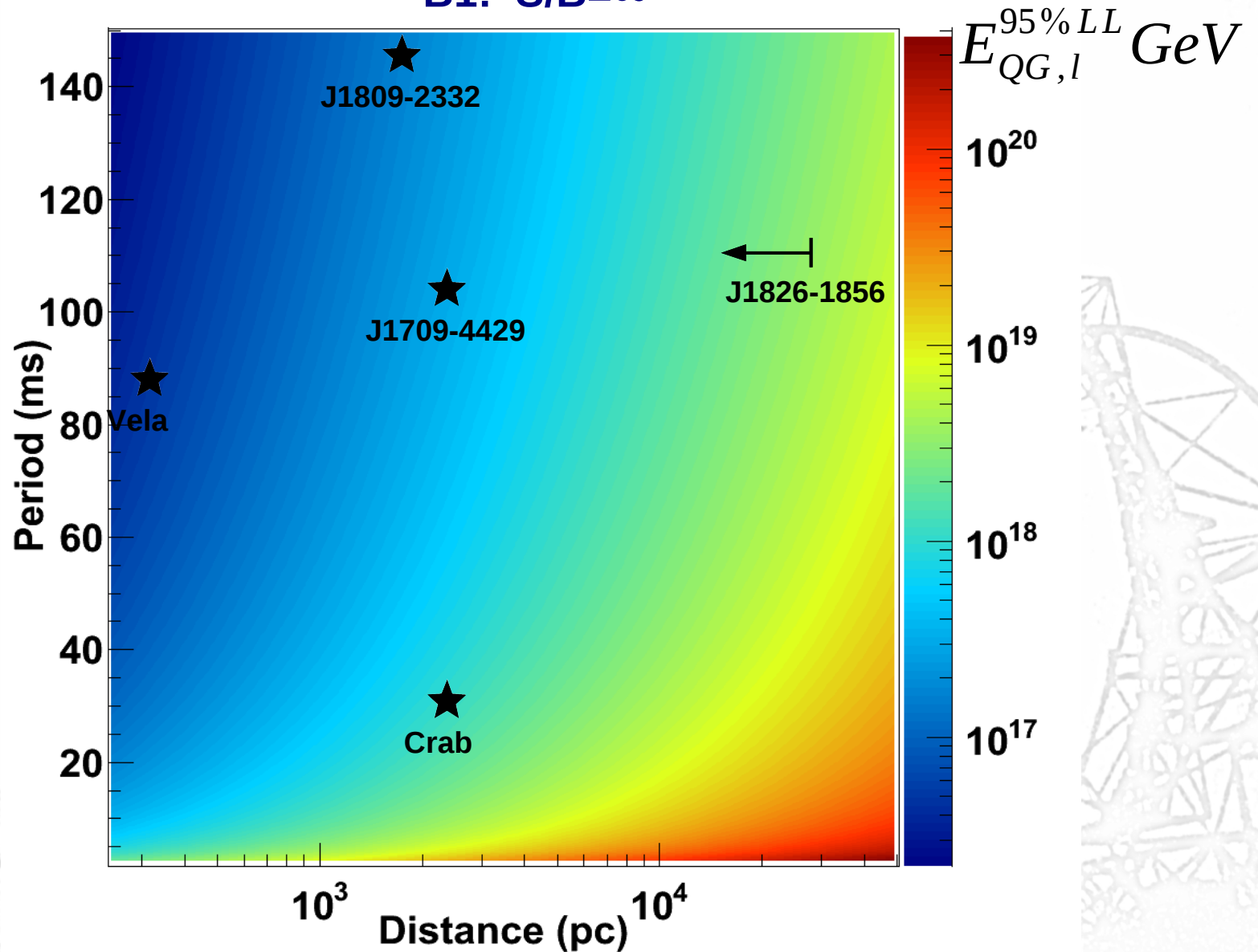
- **Improper coverage**, mainly due to:
  - Template phasogram uncertainties
  - Spectrum parametrization

- **Refine threshold** on  $-2\Delta\ln(L)$  to get proper coverage.
  - Derive **mean upper/lower limits** on linear and quadratic phase lag parameter
  - Lower limits on quantum gravity scale  $E_{QG}$

# HESS II performances with pulsars

## Sensitivity (linear correction, subluminal)

B1:  $S/B=\infty$



# HESS II performances with pulsars

$E_{\text{QG}}^{95\% \text{ LL}}$ (GeV) for H.E.S.S.2 pulsar candidates	Linear		Quadratic	
	S/B= $\infty$	S/B=1	S/B= $\infty$	S/B=1
<b>Crab</b>	$1.04 \times 10^{18}$	$5.47 \times 10^{17}$	$1.74 \times 10^{10}$	$1.48 \times 10^{10}$
<b>PSR J1826-1256*</b>	$< 3.18 \times 10^{18}$	$< 1.83 \times 10^{18}$	$< 3.19 \times 10^{10}$	$< 2.72 \times 10^{10}$
<b>PSR J1709-4429</b>	$3.19 \times 10^{17}$	$1.84 \times 10^{17}$	$1.01 \times 10^{10}$	$8.63 \times 10^9$
<b>PSR J1809-2332</b>	$1.64 \times 10^{17}$	$9.5 \times 10^{16}$	$7.25 \times 10^9$	$6.20 \times 10^9$
<b>Vela</b>	$4.69 \times 10^{16}$	$2.71 \times 10^{16}$	$3.87 \times 10^9$	$3.31 \times 10^9$

\* from published upper limit on distance (Fermi 2<sup>nd</sup> year catalog), distance to the Galaxy's edge

# HESS II performances with AGNs

## Toy MC simulations

### Modest flare from PKS 2155-304:

- 1 gaussian pulse in 25 min
- 1000 events  $> 0.3$  TeV
- $\sigma_{\text{flare}} = 250$  s
- Power law spectrum  $E^{-\Gamma}$   $\Gamma=3.2$

### Acceptance and resolution: HESS II hybrid/mono

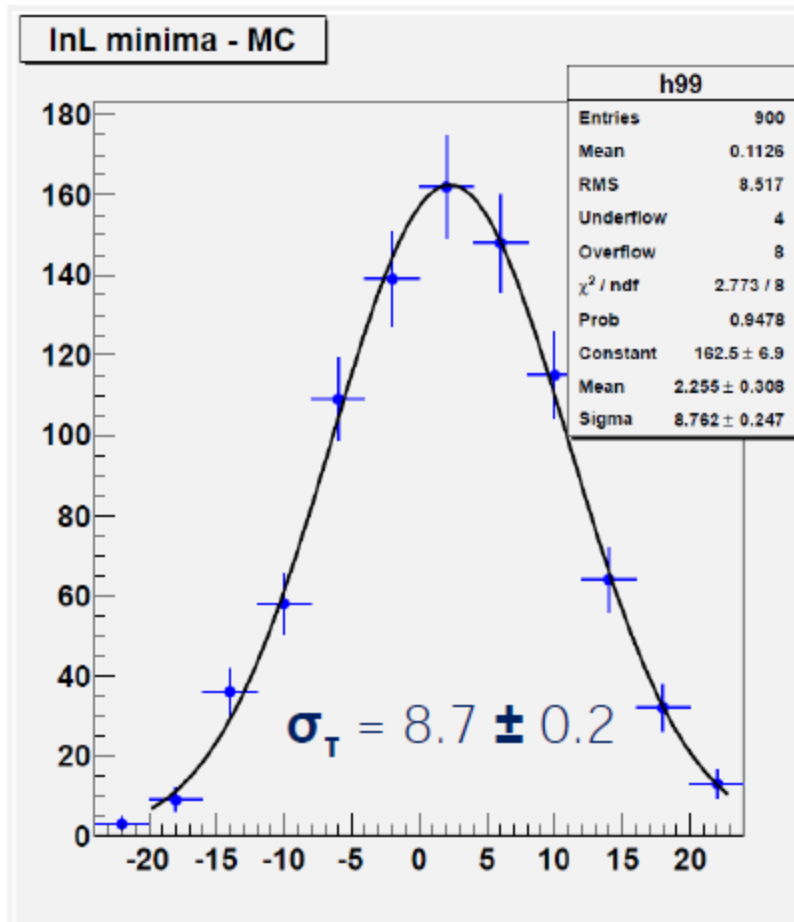
- Estimation of no of events in the low energy range for a Template LC
- HESS I/ HESS II sensitivity ratio in 0.15 – 1.0 TeV range  $\sim 2$
- Safe range for likelihood fit ( $> 0.15$  TeV) with respect to:  
Efficient background suppression  
Assuming a power law spectrum reconstruction

# HESS II performances with AGNs

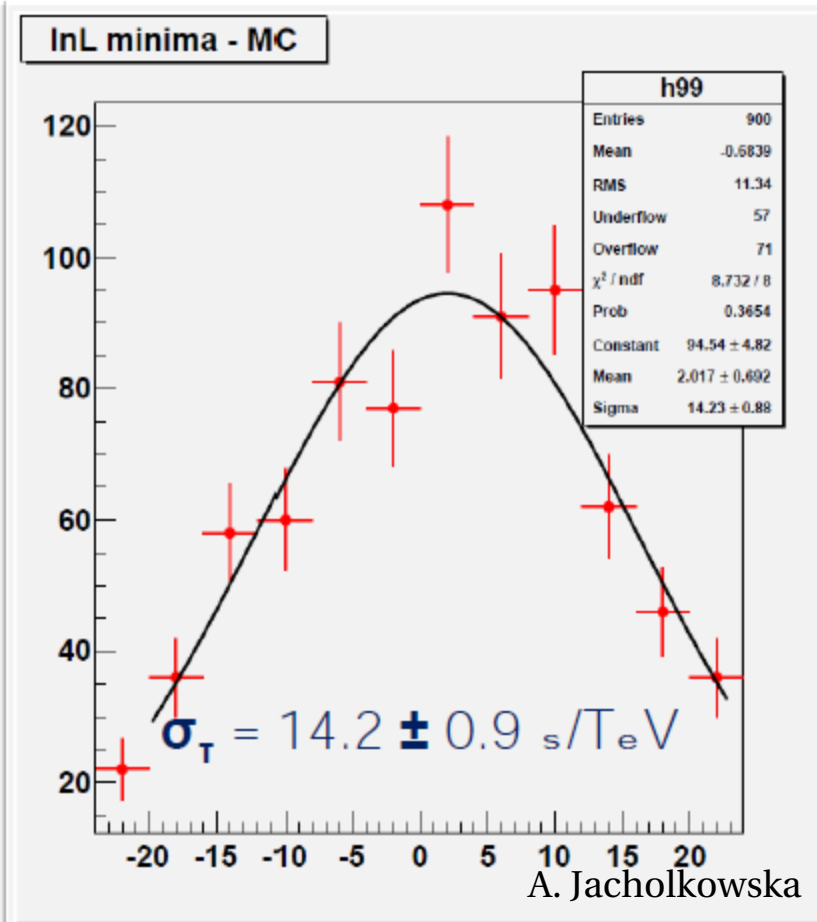
## Error calibration

- Statistical precision measurement: calibrated error p.d.f.s

HESS 1  $E > 0.3$  TeV



HESS 2 mono  $E > 0.15$  TeV

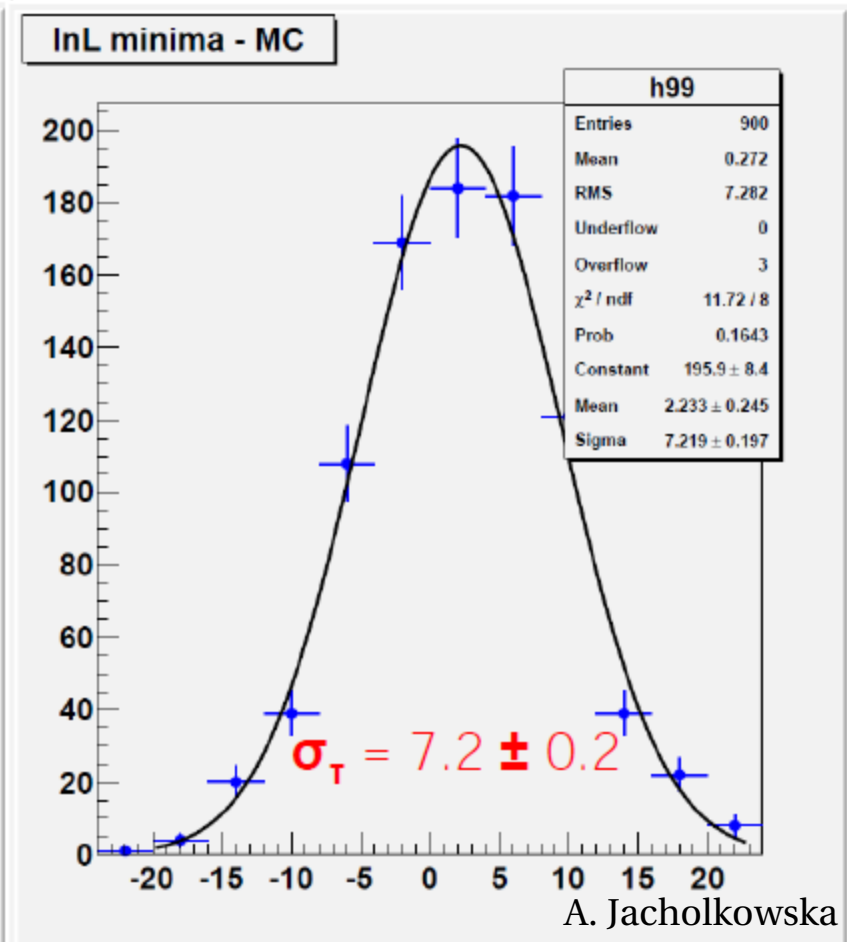
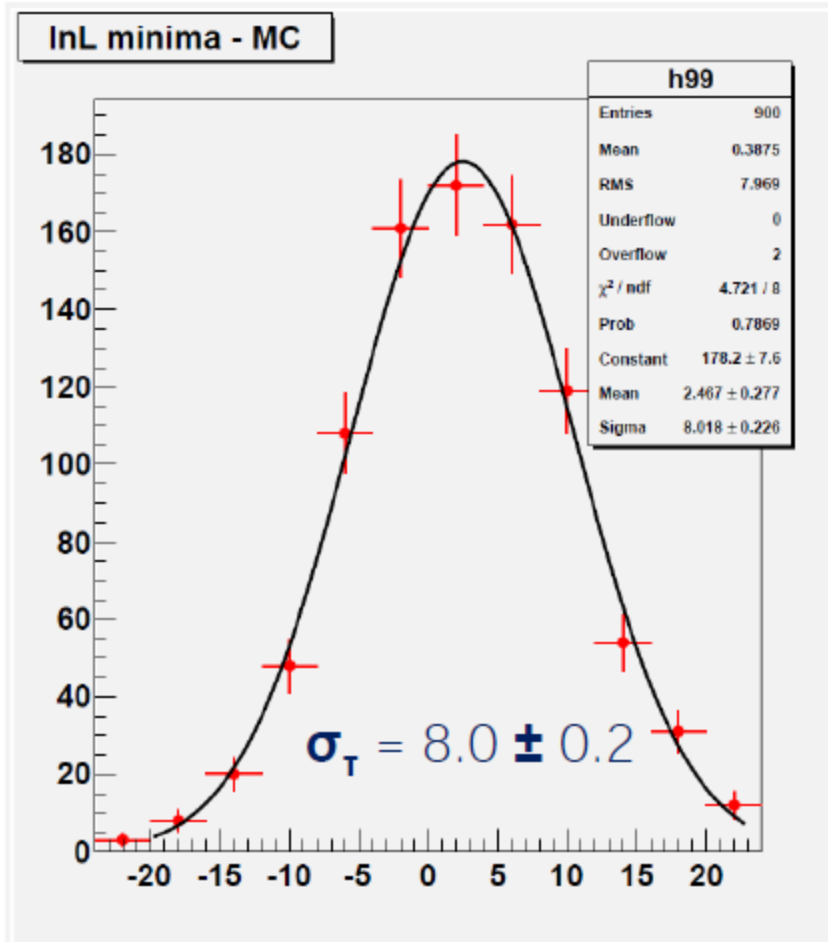


# HESS II performances with AGNs

## Error calibration

HESS 1 + HESS 2 mono

HESS 2 hybrid E > 0.2 TeV

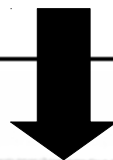


# HESS II performances with AGNs

## Summary

A. Jacholkowska

Mode	$N_{\text{evt}}$	Calibrated error $\sigma_T$ (s/TeV)	Template LC range (TeV)	Remarks
HESS 1 $E > 0.3 \text{ TeV}$	1000	$8.7 \pm 0.2$	0.15 – 0.25	Low intensity flare BF calibration: 5.5 s/TeV
HESS 2 <sub>mono</sub> $E > 0.15 \text{ TeV}$	1100	$14.2 \pm 0.9$	0.05 – 0.12	Not competitive alone
HESS 1 + HESS 2 <sub>mono</sub> $E > 0.3 \quad E > 0.15 \text{ TeV}$	2100	$8.0 \pm 0.2$	0.15 – 0.25 0.05 – 0.12	Suitable for tests: 2 template LCs
HESS 2 <sub>hybrid</sub> $E > 0.2 \text{ TeV}$	3600	$7.2 \pm 0.2$	0.05 – 0.12	error: 25% improvement



With systematics  $\sigma_{\text{syst}} \approx \sigma_{\text{stat}}$

$E_{\text{QG}}^1 > 3.50 \times 10^{18} \text{ GeV (95\% CL)}$

# Summary and Conclusions

- **Overall:**

- Increase in sensitivity  $<0.2$  TeV, better Template at low energy
- Larger statistics

- If **pulsars** confirmed with HESS II (**Mono running mode**)

- Permanent pulsations, low systematics
- “Crab like” competitors to AGNs
- With millisecond pulsars, could reach the Planck scale.

- With **AGNs** (PKS 2155-304)

- **Hybrid running mode**
- 25% improvement on statistical error compared to HESS I

- With **GRBs**

- Work is ongoing, preliminary result ( $z=0.5$ ):  $E_{\text{QG}}^1 > 1.02 \times 10^{20}$  GeV

- White paper before end of the year

# Thanks Tack!



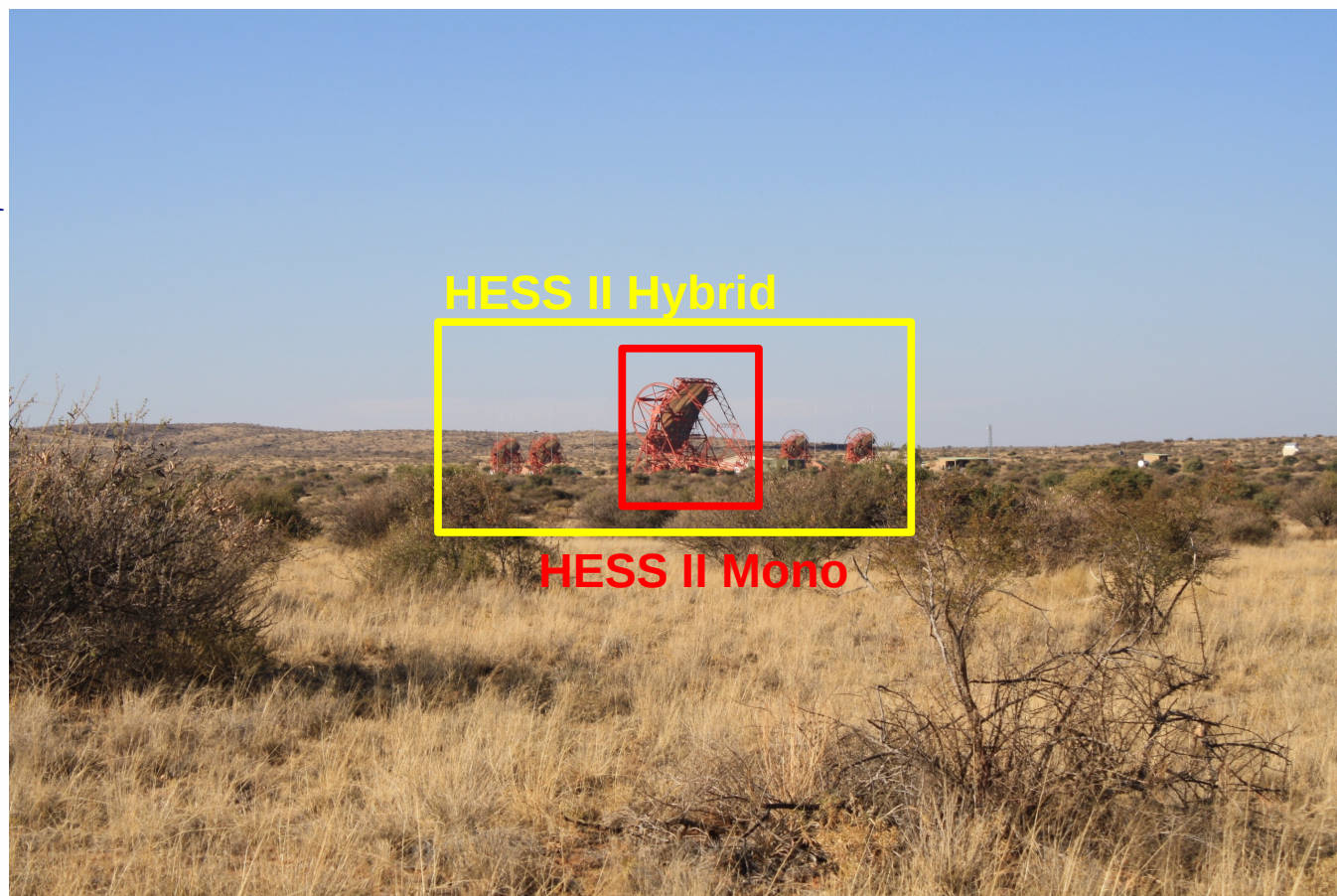
*"That's a violation of the law of Lorentz invariance, baby"*  
Futurama, "Law and Oracle" (2011)

# Backup slides

## HESS II telescope running modes

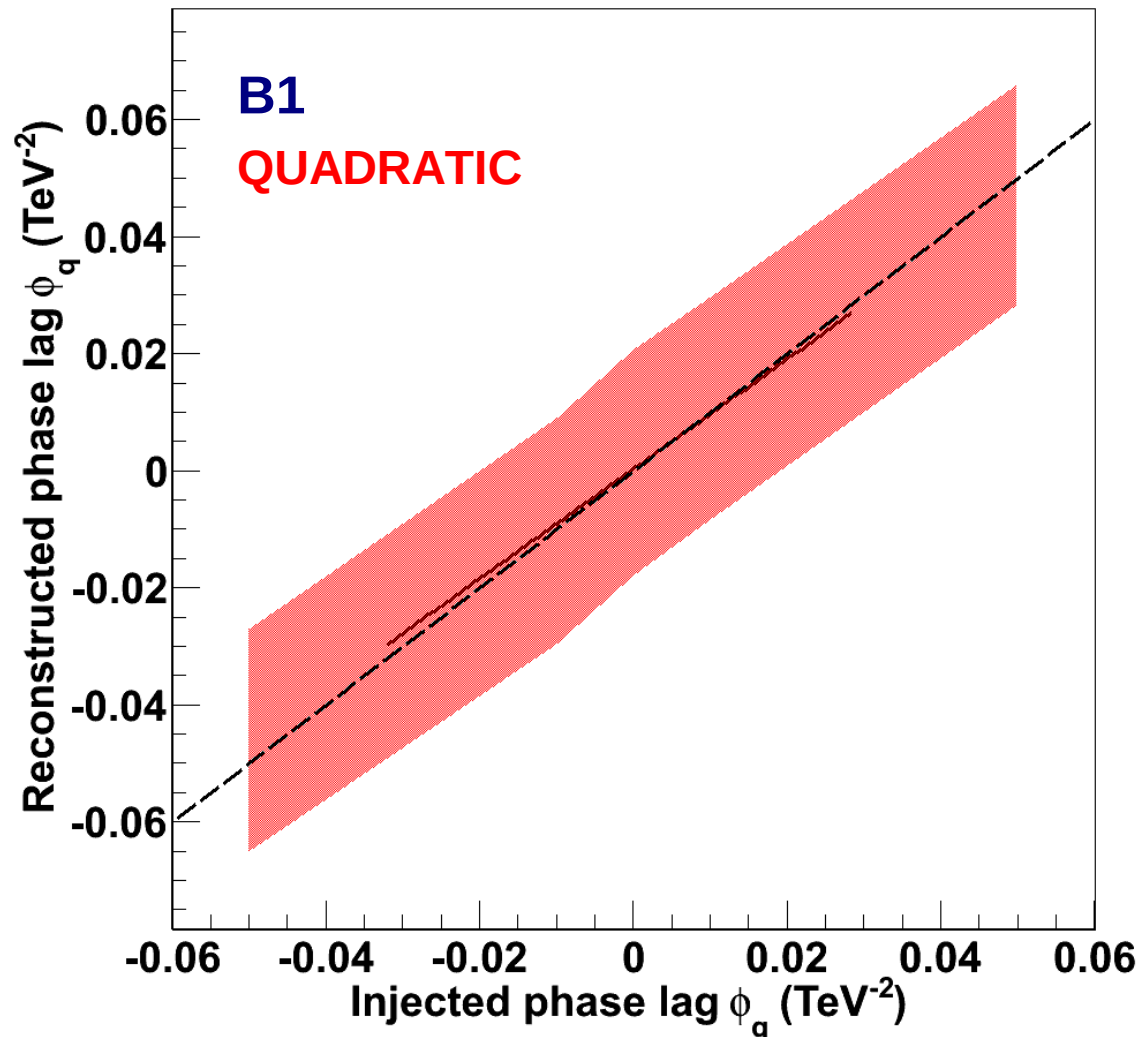
- Hybrid
  - Higher energy threshold
  - Access higher energies

- Mono
  - Lower energy threshold (smaller effective area)
  - Access lower energies ( $\sim < 100$  GeV)



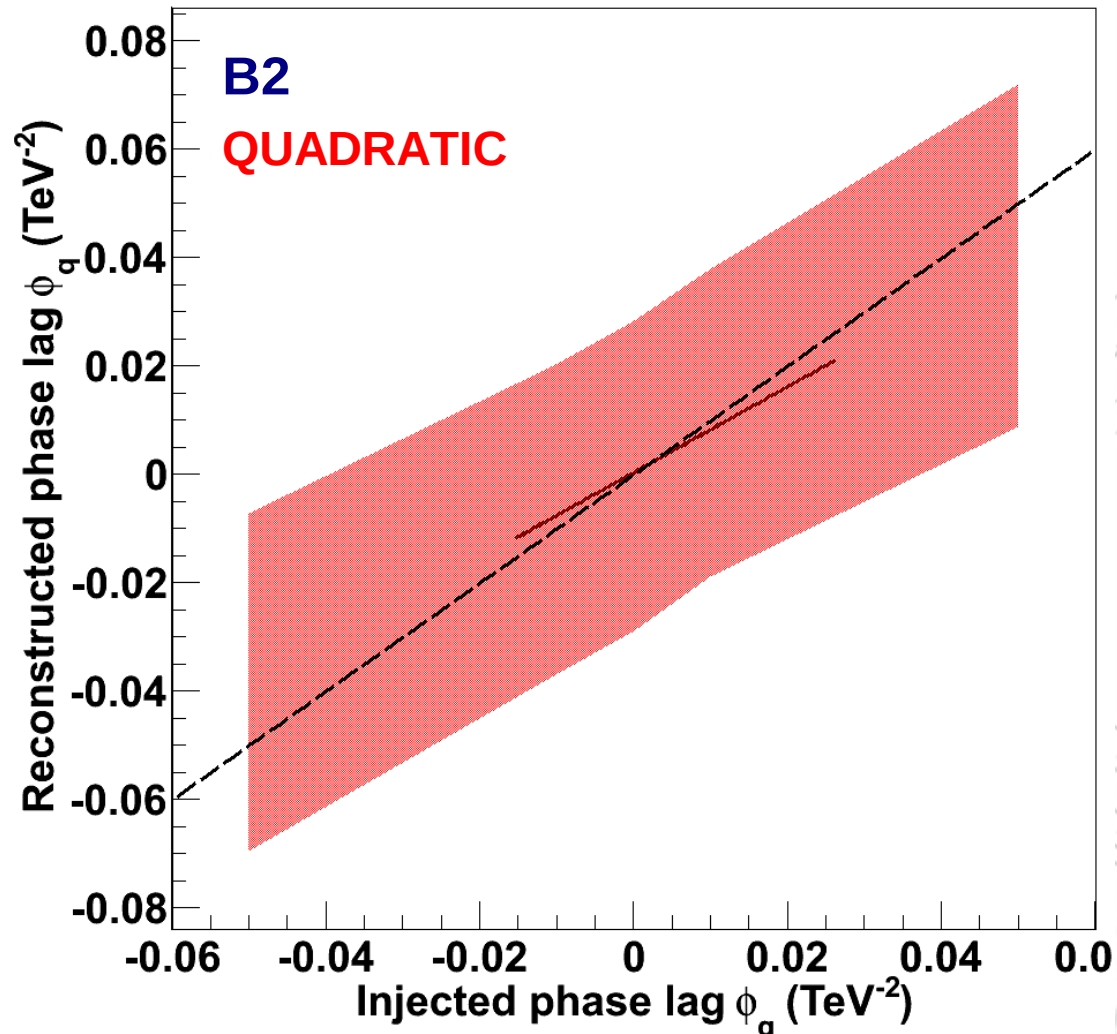
# Backup slides

## Calibration curves



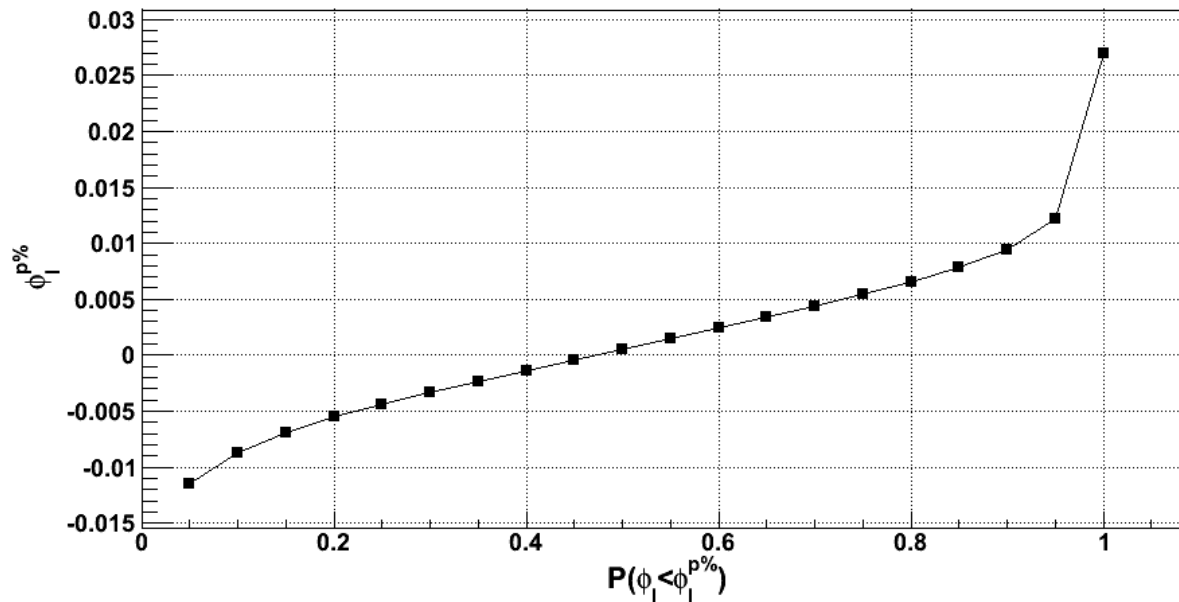
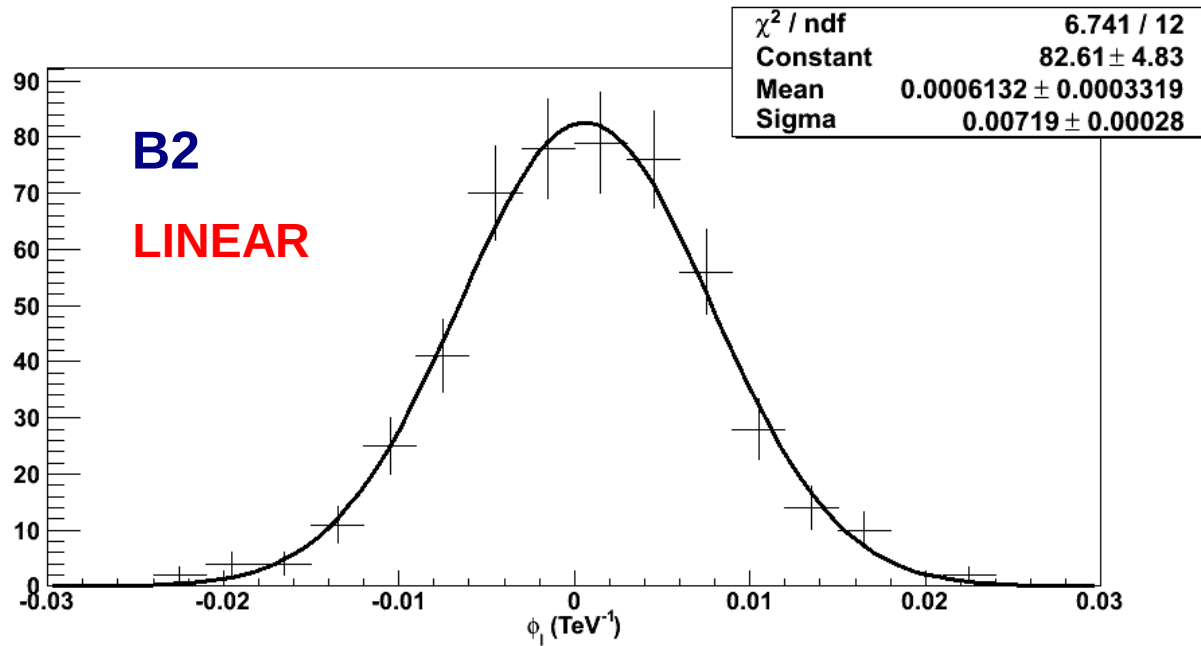
# Backup slides

## Calibration curves



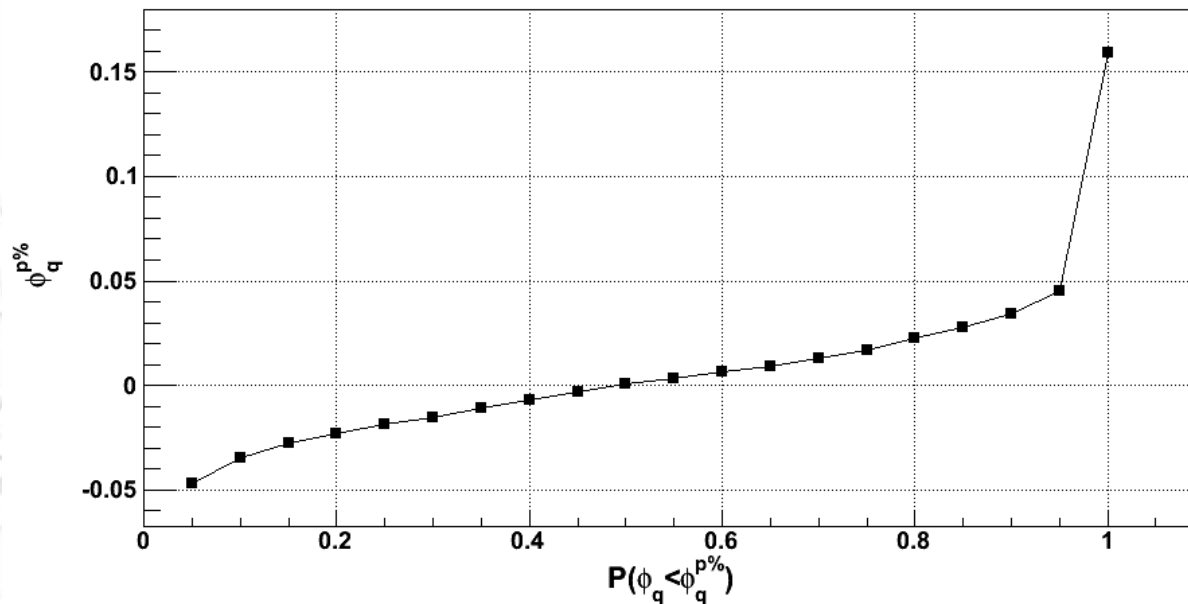
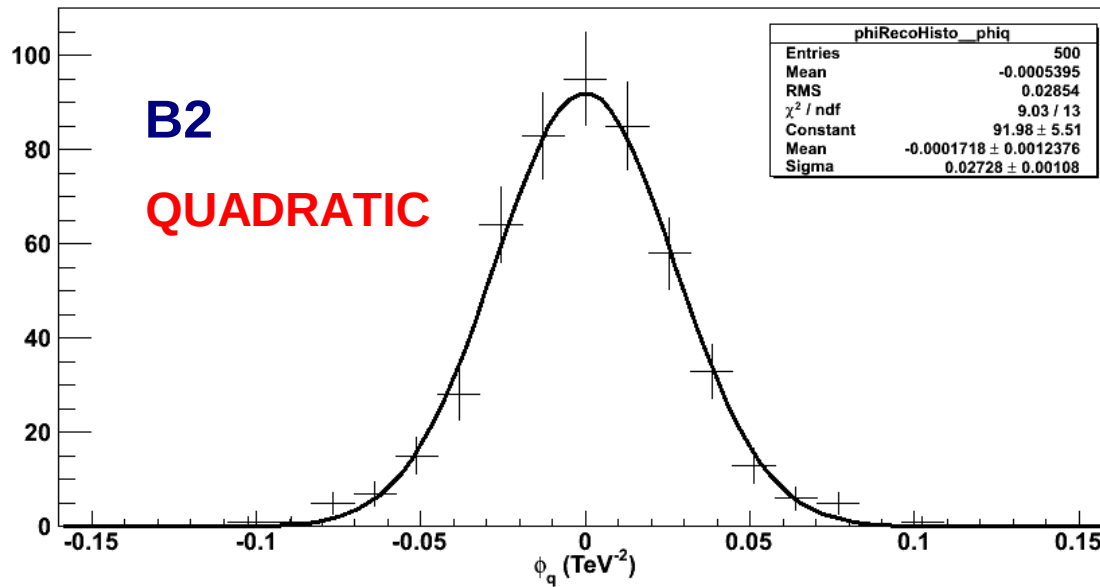
# Backup slides

## Distribution of reconstructed phase lag (no LIV)



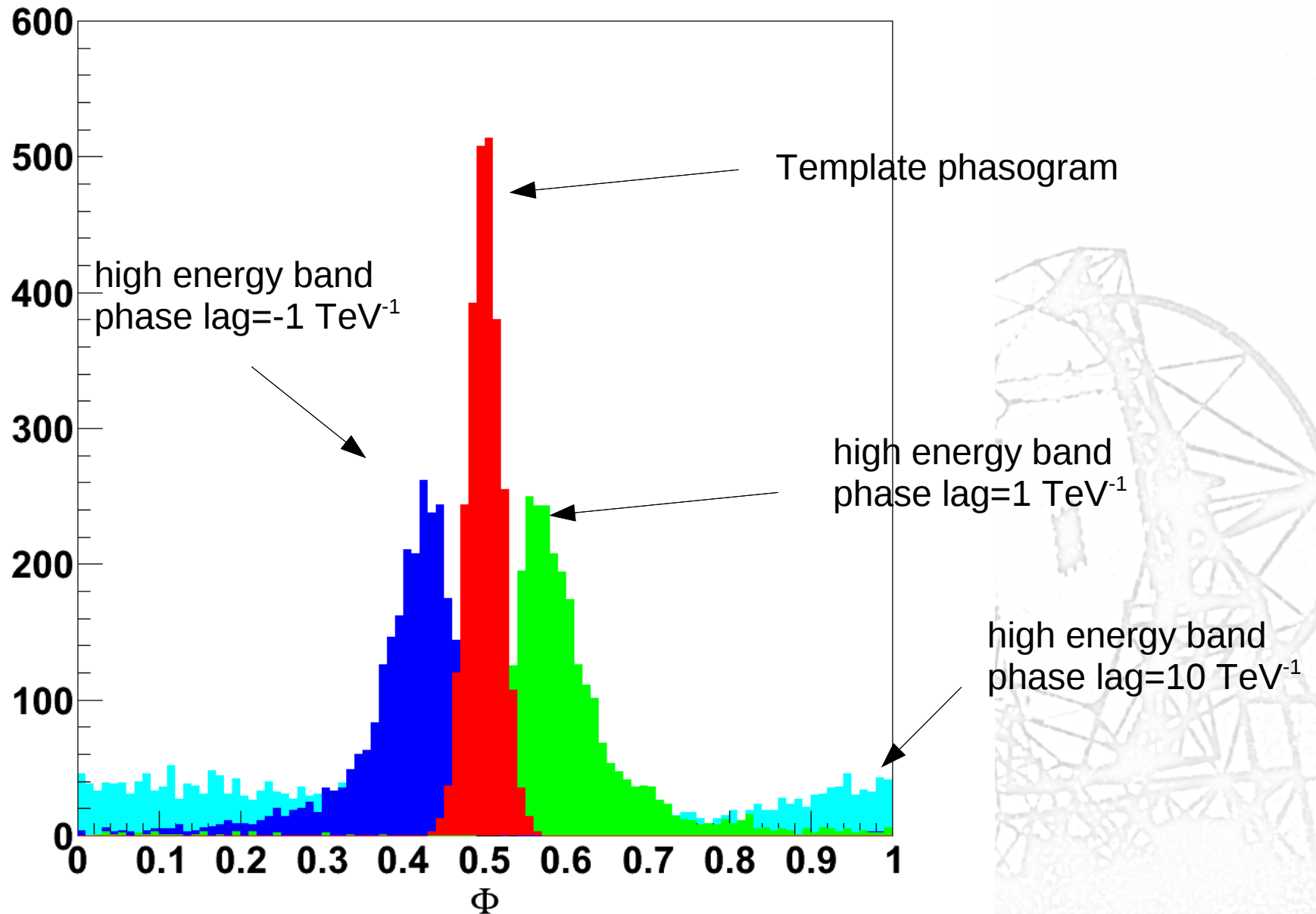
# Backup slides

## Distribution of reconstructed phase lag (no LIV)



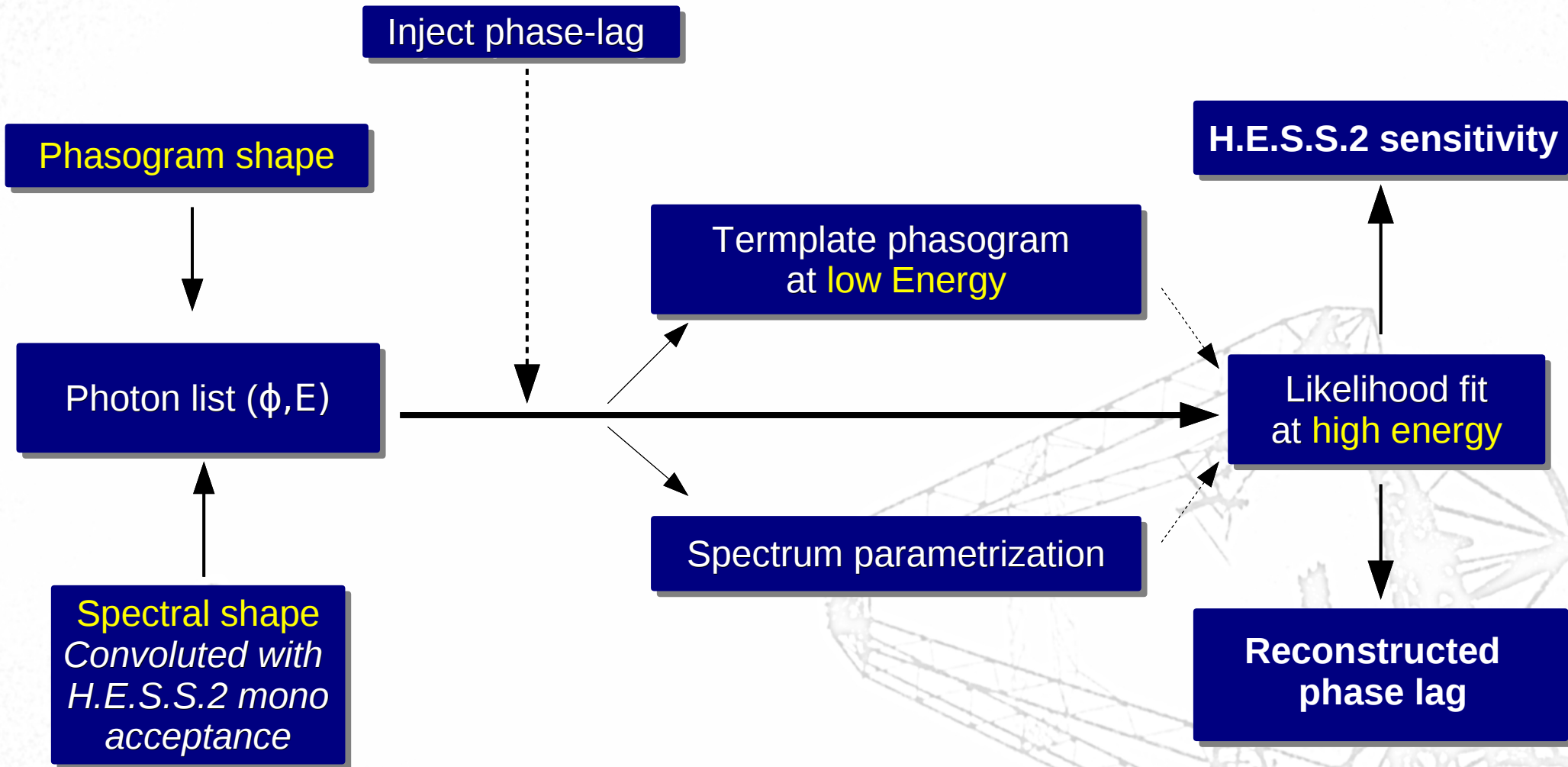
# Backup slides

## Effect of LIV on phasogram



# Backup slides

## Toy Monte Carlo (pulsars)



- Generate 500 realizations.
- Inject **phase-lag parameter** from  $-0.05$  to  $0.05 \text{ TeV}^{-1}(-^2)$ .
- 2 energy intervals: **low energy** (30 – 55 GeV) and **high energy** (55 GeV – 1 TeV)

# Backup slides

## Pulsar candidates for HESS II

Name (PSR)	zenith <sub>culm</sub> (°)	log <sub>10</sub> (F <sub>10–100GeV</sub> ) (cm <sup>-2</sup> s <sup>-1</sup> )	log <sub>10</sub> (F <sub>1–100GeV</sub> ) [2] (cm <sup>-2</sup> s <sup>-1</sup> )	Δβ
<b>J0835-4510*</b>	22	-8.01	-5.87	—
<b>J1709-4429</b>	21	-8.63	-6.72	3.20-3.70
<b>J1809-2332</b>	0	-9.28	-7.16	3.50-3.70
J1907+0602	29	-9.47	-7.42	2.90-3.50
<b>J1826-1256</b>	10	-9.51	-7.27	3.00-3.60
J1732-3131	8	-9.57	-7.43	3.10-3.50
J1833-1034	13	-9.63	-7.99	2.30-2.70
J0633+0632	30	-9.72	-7.81	3.00-3.10
J1614-2230	1	-10.11	-8.34	2.60-2.70
J2124-3358	11	-10.16	-8.13	2.10-2.30

Table 1: Top-ten list of the best candidates to reach  $5\sigma$  in 100 hours for observation zenith angles  $<30^\circ$ . The columns represent (by left-right order): the source culmination zenith angle, the logarithm of the energy flux between 1 and 100 GeV ( $F_{1-100\text{ GeV}}$  for Crab pulsar is  $1.8 \times 10^{-7} \text{ cm}^{-2} \text{ s}^{-1}$ ) and the range of values in  $\beta$  allowed in our simulation for each pulsar. The asterisk (\*) following Vela pulsar's name indicates that it is the top-ten list besides of having a strong indication of an exponential cut-off at high energies, since it is the most energetic one in the Southern hemisphere.

# Backup slides

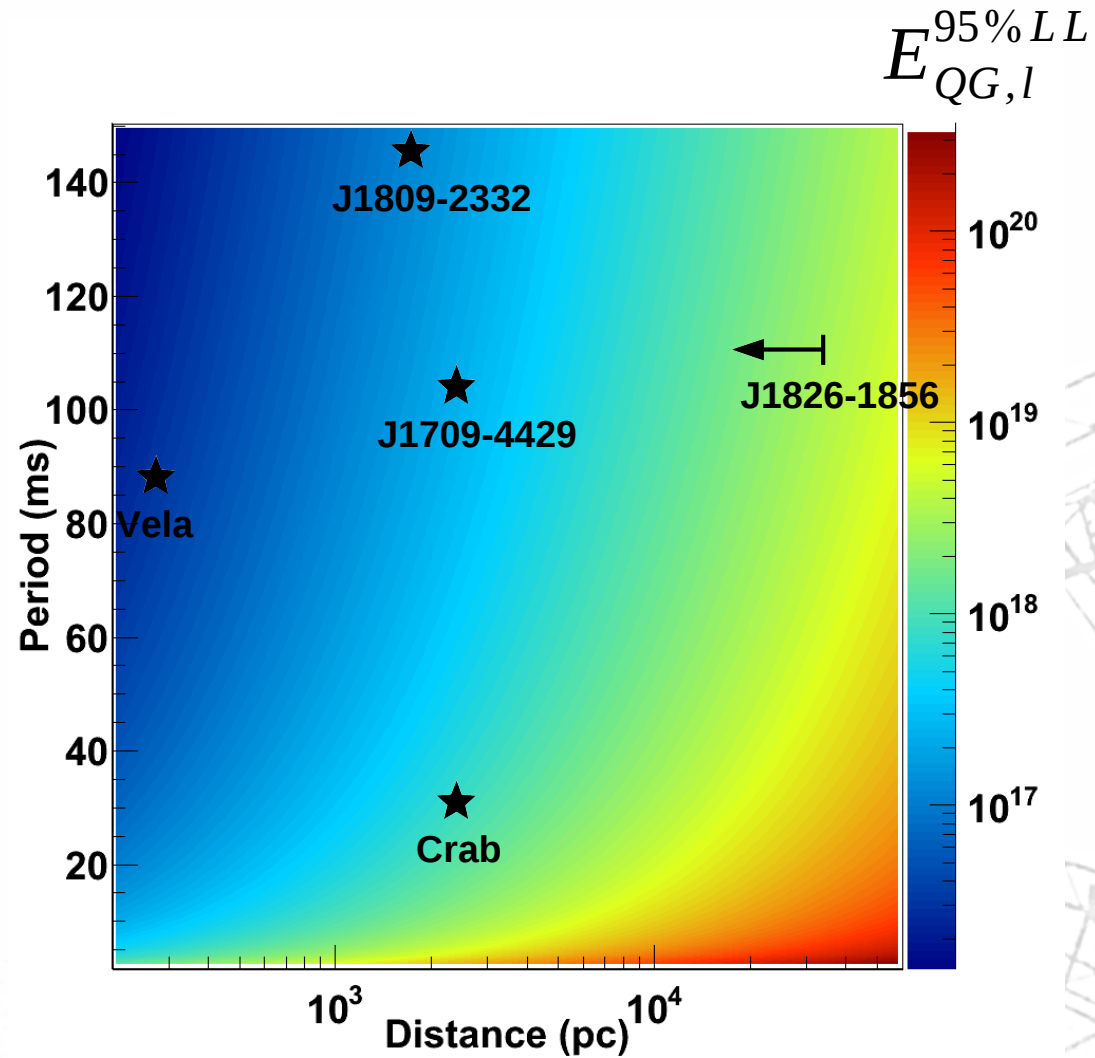
## 6 Fermi millisecond pulsars

Pulsar name	$l, b$	$P$ (ms)	$d$ (pc)	$\text{Log } \dot{E}$ ( $\text{ergs s}^{-1}$ )	$\delta$	$\Delta$	Photon flux >0.1 GeV ( $10^{-8}$ photons $\text{cm}^{-2} \text{s}^{-1}$ )	Energy flux >0.1 GeV ( $10^{-11}$ ergs $\text{cm}^{-2} \text{s}^{-1}$ )	Spectral index	Exponential cutoff energy (GeV)	$\eta$ (%)
J0030+0451	113.1°, -57.6°	4.865	300 ± 90	33.54	0.16	0.45	5.5 ± 0.7	4.9 ± 0.3	1.3 ± 0.2	1.9 ± 0.4	15 ± 9
J0218+4232 (b)	139.5°, -17.5°	2.323	2700 ± 600*	35.39	0.50	—	5.6 ± 1.3	3.5 ± 0.5	2.0 ± 0.2	7 ± 4	13 ± 6
J0437-4715 (b)	253.4°, -42.0°	5.757	156 ± 2	33.46	0.45	—	4.4 ± 1.0	1.9 ± 0.3	2.1 ± 0.3	2.1 ± 1.1	1.9 ± 0.3
J0613-0200 (b)	210.4°, -9.3°	3.061	480 ± 140	34.10	0.42	—	3.1 ± 0.7	3.1 ± 0.3	1.4 ± 0.2	2.9 ± 0.7	7 ± 4
J0751+1807 (b)	202.7°, 21.1°	3.479	620 ± 310	33.85	0.42	—	2.0 ± 0.7	1.7 ± 0.2	1.6 ± 0.2	3.4 ± 1.2	11 ± 11
J1614-2230 (b)	352.5°, 20.3°	3.151	1300 ± 250*	33.7	0.20	0.48	2.3 ± 2.1	2.5 ± 0.8	1.0 ± 0.3	1.2 ± 0.5	100 ± 80
J1744-1134	14.8°, 9.2°	4.075	470 ± 90	33.60	0.85	—	7.1 ± 1.4	4.0 ± 1.0	1.5 ± 0.2	1.1 ± 0.2	27 ± 12
J2124-3358	10.9°, -45.4°	4.931	250 ± 125	33.6	0.85	—	2.9 ± 0.5	3.4 ± 0.3	1.3 ± 0.2	2.9 ± 0.9	6 ± 6

A. A. Abdo *et al.*  
*Science* **325**, 848 (2009);

# Backup slides

## Sensitivity (linear correction)

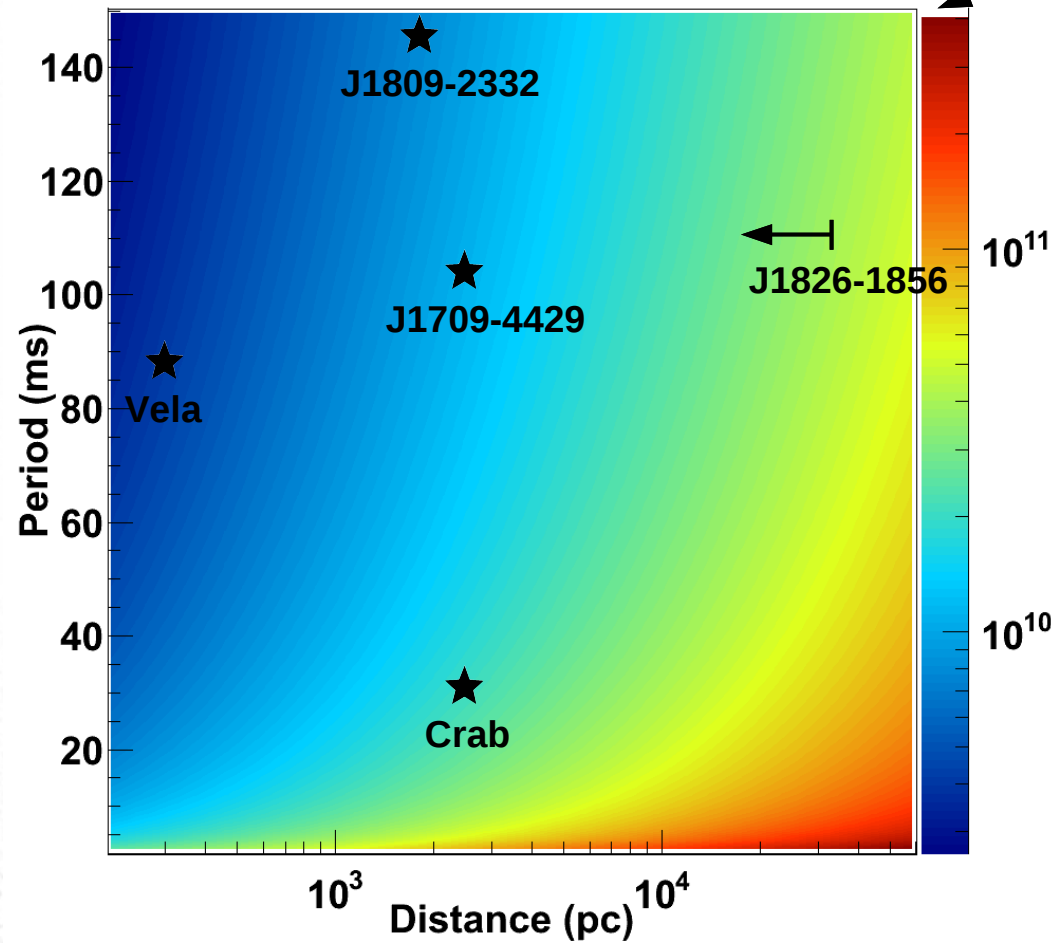


**B2: S/B=1**

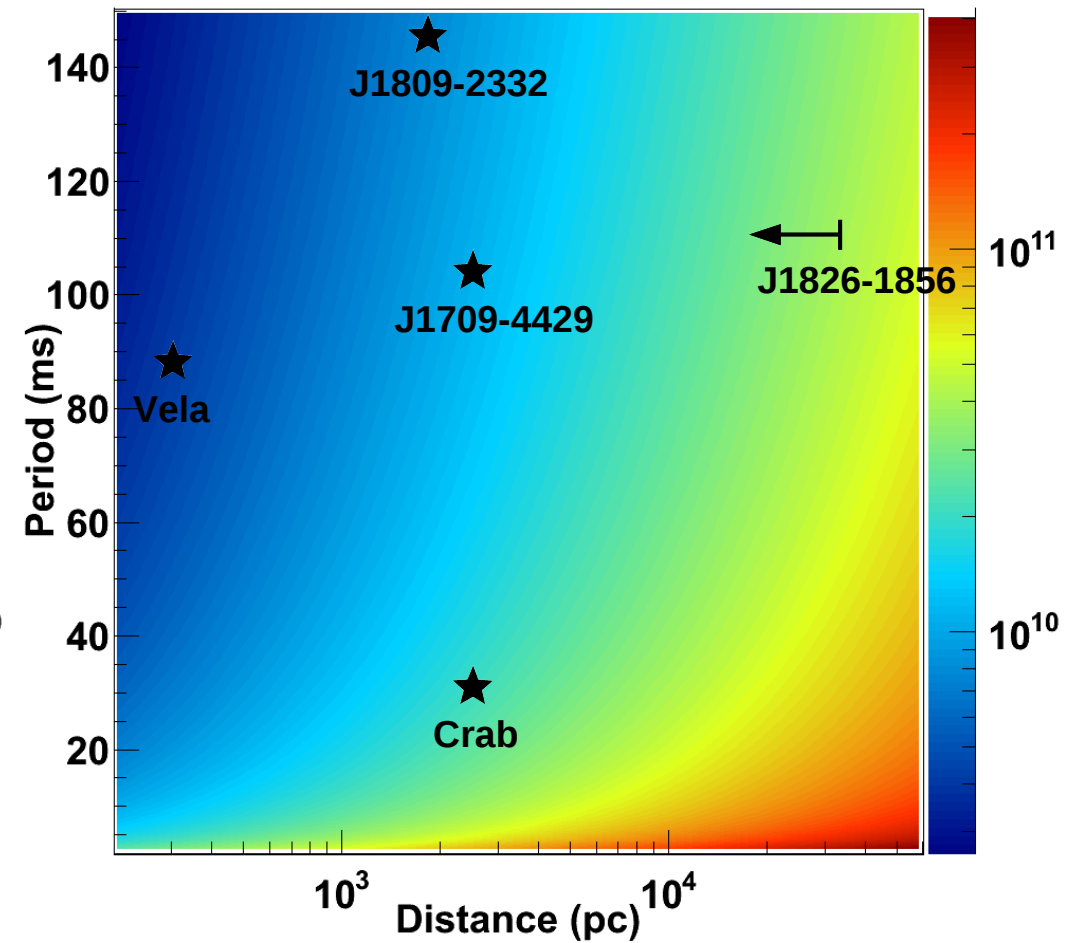
# Backup slides

## Quadratic term

$$E_{QG,q}^{95\%LL}$$



**B1:  $S/B = \infty$**



**B2:  $S/B = 1$**

# Backup slides

## Distinguish between LIV and source intrinsic delays

- **LIV delay:**

- $P(t) = P + dP/dt t$  and  $\Delta\Phi(t) = \Delta t / P(t)$  in pulsar frame
- $\Delta\Phi$  decreases with time for LIV delays.

- **Source Intrinsic delay:**

- $\Delta\Phi = \text{Constant}$  in pulsar frame (if not correlated with period increase)
- No change with time

